

## Oxygen-Stabilized Rh Adatoms: 0D Oxides on a Vicinal Surface

Florian Mittendorfer,<sup>†</sup> Thomas Franz,<sup>‡</sup> Jan Klikovits,<sup>†</sup> Michael Schmid,<sup>\*,†</sup> Lindsay R. Merte,<sup>†,§</sup> Sameena Shah Zaman,<sup>†</sup> Peter Varga,<sup>†</sup> Rasmus Westerström,<sup>¶</sup> Andrea Resta,<sup>¶,||</sup> Jesper N. Andersen,<sup>¶</sup> Johan Gustafson,<sup>¶</sup> and Edvin Lundgren<sup>¶</sup>

<sup>†</sup>Institut für Angewandte Physik, Technische Universität Wien, 1040 Wien, Austria

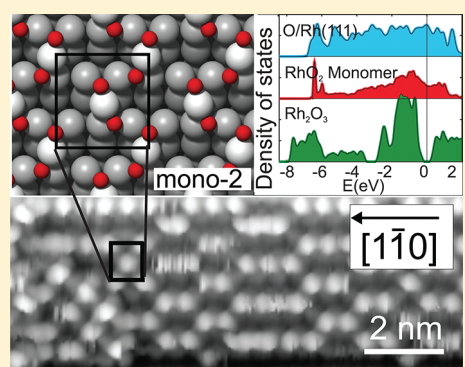
<sup>‡</sup>Faculty of Physics and Center for Computational Materials Science, University of Vienna, 1090 Wien, Austria

<sup>¶</sup>Division of Synchrotron Radiation Research, Lund University, Box 118, S-22100 Sweden

Supporting Information

**ABSTRACT:** We have investigated the initial oxidation of the Rh(113) and Rh(223) vicinal surfaces by STM and ab initio simulations. Upon adsorption of small amounts of oxygen, the surface morphology is completely altered. Surprisingly, oxygen-stabilized Rh adatoms can be observed on the (113) facets, with oxide-like electronic properties. We present models of these “0D oxide” phases and discuss reasons for their stability.

**SECTION:** Surfaces, Interfaces, Catalysis



Understanding surface reactions at the atomic level is of both fundamental and applied interest in areas as diverse as heterogeneous catalysis and corrosion protection. Oxidation processes at surfaces are particularly important, and it is well-known that the oxidation state of a metal catalyst's surface strongly affects the catalytic behavior. It has been reported that oxidized surfaces of Pt,<sup>1,2</sup> Pd,<sup>3,4</sup> Rh,<sup>5–7</sup> PtRh,<sup>8</sup> Ru,<sup>9,10</sup> and nanoparticles<sup>11,12</sup> are more efficient in the catalytic oxidation of CO than the pure metal surface. Although these reports have been disputed,<sup>13</sup> it becomes increasingly clear that the simple picture of adsorption and reaction of atoms on an unmodified substrate is inadequate in many cases, even for the noble metals of the Pt group, and more information on the surface chemistry of catalytically active metals like Rh is clearly needed.

It has also turned out that understanding only low-index (close packed) single-crystal surfaces is often insufficient because steps can be the active sites for many reaction steps.<sup>14,15</sup> Vicinal surfaces, that is, surfaces with orientations different from the low-index directions and with a high step density, provide a bridge over the materials gap between low-index surfaces and nanoparticles or other “real-world” surfaces. It has been shown previously that oxygen adsorption at vicinal surfaces often leads to formation of terraces (facets) with different orientations,<sup>16,17</sup> but otherwise, the structures observed were as expected, with O atoms at the steps bound in essentially the same sites as those on the terraces of low-index surfaces.<sup>16–20</sup> With exposure to increasing amounts of oxygen, the structures formed at the steps can be considered one-dimensional (1D) oxides<sup>19</sup> and then 2D oxides

(surface oxides) on the terraces, and finally, 3D oxidation of the bulk material sets in.

In this Letter, we report scanning tunneling microscopy (STM) and density functional theory (DFT) results on a new phenomenon related to oxidation, the formation of Rh adatoms forming RhO<sub>2</sub> entities on a vicinal surface. In analogy to 2D and 1D oxides, we call them “0D oxides” because the electronic structure shows clear signs of an oxide, and also, the local bonding geometry of the Rh adatoms is governed by the oxygen. We find that very small amounts of oxygen are sufficient to induce this transformation, less than what would be required for formation of a 1D oxide at steps; therefore, with increasing oxygen coverage, the surface proceeds from 0D via 1D and 2D to 3D oxides. The significance of the 0D oxides is also emphasized by the observation that oxidation also causes the flatter Rh(223) surface (and probably many similar vicinal surfaces) to completely rearrange, forming (113) facets hosting the 0D oxide. With their undercoordinated Rh atoms, we believe that these 0D oxides will be highly reactive, more reactive than any of the Rh bulk oxides (RhO<sub>2</sub>, Rh<sub>2</sub>O<sub>3</sub>) and the 2D surface oxide of Rh, which reacts at edges and defects only.<sup>21</sup>

STM images were recorded in Vienna using a two-chamber ultrahigh vacuum system with a pressure below  $1 \times 10^{-10}$  mbar, using the same STM as in refs 19, 22, and 23. The STM was

**Received:** August 19, 2011

**Accepted:** October 11, 2011

**Published:** October 11, 2011

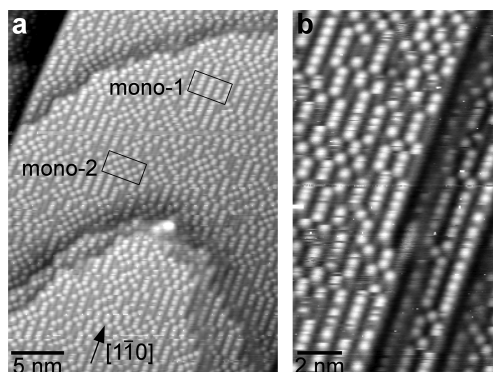


**Figure 1.** (a, b) STM images ( $V_{\text{sample}} = -0.4$  and  $-1.2$  V,  $0.1$  nA; slightly high-pass filtered) of a Rh(113) sample after exposure to  $0.3$  L of oxygen at  $300$  °C.

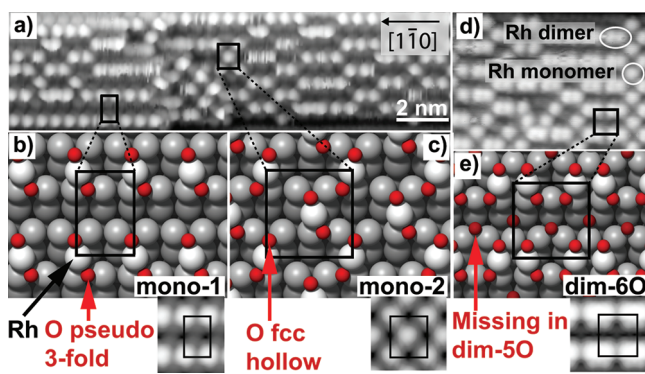


**Figure 2.** STM images of (113) faceted areas of a Rh(223) sample with (a) Rh ad-monomers stabilized by oxygen after an exposure of  $1$  L ( $-2$  mV,  $2.6$  nA) and (d) also showing ad-dimers after an exposure of  $9$  L of oxygen ( $-1$  V,  $0.52$  nA). Structure models (b, c, e) are based on our DFT calculations, with the corresponding STM simulations shown below. The black rectangles show the unit cells, with dimensions of  $0.54 \times 0.89$  nm $^2$  in (b) and  $0.81 \times 0.89$  nm $^2$  in (c, d, e).

operated in constant current mode at room temperature. The Rh(113) and Rh(223) crystals were cleaned by cycles of Ar<sup>+</sup> sputtering and annealing to  $850$  °C, occasional oxygen treatments at temperatures up to  $825$  °C in order to remove residual C, and a short anneal in vacuum up to  $950$  °C in order to remove adsorbed O. Thereafter, Auger electron spectroscopy did not show any contaminants such as C and O. For oxidation, O<sub>2</sub> was dosed at a sample temperature between  $300$  and  $450$  °C with a pressure between  $5 \times 10^{-9}$  and  $1 \times 10^{-8}$  mbar.

The calculations were performed with the Vienna ab initio simulation package (VASP),<sup>24,25</sup> using PAW potentials,<sup>26,27</sup> the PW91 exchange–correlation functional,<sup>28</sup> and a cutoff energy of  $250$  eV. The surfaces were modeled by a slab consisting of six layers parallel to the (111) terraces with relaxation of the upper two layers. For the Rh(113) surface, a  $k$ -point mesh corresponding to a  $24 \times 16 \times 1$  mesh for the primitive cell was used. The Bader analysis was performed with the Bader code.<sup>29,30</sup>

Figure 1 shows a STM image of the Rh(113) vicinal surface after an oxygen exposure of  $0.3$  L (1 Langmuir =  $1$  s at  $1 \times 10^{-6}$  Torr). The image displays bright protrusions with two different types of ordering, named “mono-1” and “mono-2”. Experiments with different oxygen coverages show that the area ratio between the mono-2 and mono-1 phases increases with increasing oxygen

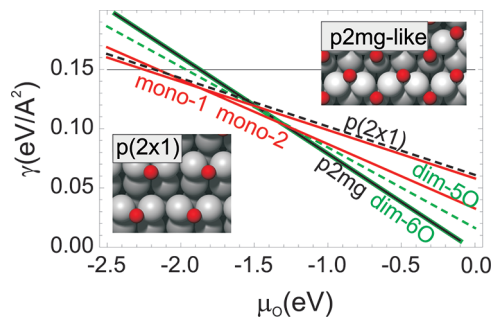


**Figure 3.** Phase diagram showing the surface free energy  $\gamma$  for oxygen on a Rh(113) surface. The lowest line in the phase diagram is the most stable structure for each value of the chemical potential; the horizontal line is for clean Rh(113). The structure dim-5O is equal to dim-6O (Figure 2e) except for one O adatom/cell missing in dim-5O. Models of the  $p(2 \times 1)$  and  $p2mg$ -like simple adsorption structures are also shown (red balls are oxygen).

coverage, that is, the mono-2 phase is more oxygen rich. The apparent height of the protrusions is  $\sim 125$  pm, almost an order of magnitude more than what would be expected for density-of-states variations induced by oxygen. Comparing this value to the geometric height of a Rh adatom on a (113) surface (115 pm) indicates that the protrusions correspond to Rh adatoms (monomers) sitting directly at the Rh(113) steps. This interpretation is also supported by the fact that the protrusions do not sit on the step edges (ridges weakly visible in small areas without protrusions in Figure 1b) but between them; see the structure model in Figure 2. The details of their atomic arrangement will be discussed below. With further increasing oxygen exposure, in addition to the single Rh adatoms discussed so far, we observe Rh ad-dimers on the (113) sample, as shown in Figure 2d,e.

The same structures also form on a Rh(223) surface, which displays the same step orientation but wider terraces. Both STM images of the clean Rh(223) surface and low-energy electron diffraction (LEED) measurements confirm that the bare Rh(223) terrace does not reconstruct but rather displays the ideal terrace width of  $11$  Å [see Supporting Information (SI)]. Yet, at oxygen doses around  $0.5$  L, if the temperature is sufficient for mobility of the substrate atoms, the surface reconstructs, and areas with (111) terraces and larger (113) facets are formed on the surface (see SI); the average (223) orientation remains unchanged. The structures on the (113) facets of the Rh(223) sample are exactly the same as those discussed above; actually, the STM images in Figure 2 were taken on such a sample.

In order to understand the occurrence of the Rh adatoms and the details of the structure, we have performed DFT calculations for varying oxygen and Rh adatom coverages. The energetically favored adatom phases are shown as models together with the corresponding STM simulations in Figure 2b,c,e. Two oxygen atoms stabilize each Rh ad-monomer, forming a RhO<sub>2</sub> unit, while the remaining parts of the (113) facet are oxygen-free. It should be noted that these structures have oxygen coverages of  $1/2$  and  $2/3$  ML on the (113) surface, which corresponds to  $4.2 \times 10^{18}$  and  $5.6 \times 10^{18}$  atoms m $^{-2}$ , respectively. These densities would correspond to  $1/4$  and  $1/3$  ML on a (111) surface; thus, the RhO<sub>2</sub> units on Rh(113) are already formed at low oxygen coverage, where only simple adsorption phases would be found on flat Rh surfaces, far below the realm of surface or bulk oxide formation.

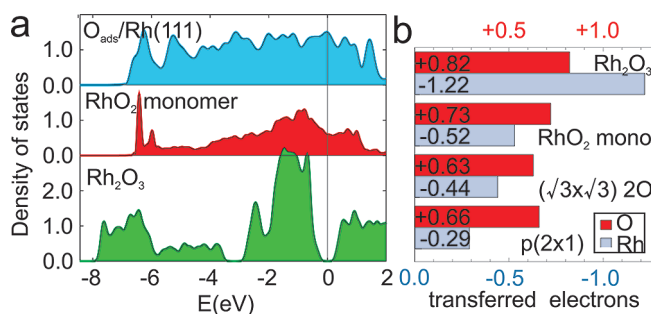


**Figure 4.** Comparison of the electronic properties. (a) Local DOS projected on the Rh atoms binding to oxygen for the  $(\sqrt{3} \times \sqrt{3})$ -2O oxygen adsorption structure, the RhO<sub>2</sub> monomers, and bulk Rh<sub>2</sub>O<sub>3</sub>. (b) Transferred electrons in these structures and in the  $p(2 \times 1)$  from Figure 3.

The ad-dimers can be considered the result of coalescence of two RhO<sub>2</sub> monomers. In addition, in the ad-dimer structure, there is space on the (111) terrace for one or two oxygen adatoms per  $(3 \times 2)$  cell (Figure 2e). Thus, by the formation of ad-dimers instead of ad-monomers, a further increase of the oxygen coverage up to 5/6 or 1 ML can be achieved. The distance between the two Rh adatoms in the ad-dimer, 3.05 Å, is close to that in the surface oxide on Rh(111) (3.02 Å<sup>22</sup>) but clearly different from metallic Rh (2.69 Å), indicating oxide-like properties of the O-stabilized Rh adatoms.

The calculated adsorption energies allow prediction of the phase diagram for oxygen on the Rh(113) surface, and the result is shown in Figure 3. For each value of the chemical potential  $\mu_O$ , the bottommost line represents the most stable structure, while the dashed lines indicate structures that cannot become thermodynamically stable at any value of  $\mu_O$ <sup>20,31</sup> (see also the SI). The calculations indeed show that the RhO<sub>2</sub> monomers and dimers are more favorable than a mere oxygen adsorption over a wide range of  $\mu_O$ . The glancing intersection of the lines in the phase diagram implies low energy differences of these structures over a wide range of the oxygen chemical potential; thus, it is not astonishing that we usually find a coexistence of these structures in our STM images of Rh(113) and the (113) facets of Rh(223) (Figures 1 and 2). At higher values of  $\mu_O$ , the energy difference between the densest dimer phase and the  $p2mg$ -like adsorption structure (named such because of its zigzag arrangement of oxygen at the Rh ridges; Figure 3) vanishes, and we have actually observed this  $p2mg$ -like structure at higher oxygen coverage by STM.

When analyzing the density of states (DOS) of the oxygen-stabilized Rh adatoms, Figure 4a, we note that they do not exhibit a wide d band with roughly constant DOS like Rh in a metal but a clear splitting into two states, a broad one around  $E_F - 1$  eV and a sharp one between -6 and -7 eV. For comparison, Figure 4 shows the DOS of Rh in bulk Rh<sub>2</sub>O<sub>3</sub> and in a structure where oxygen is merely adsorbed on a Rh(111) surface. For the latter, we have chosen a  $(\sqrt{3} \times \sqrt{3})R30^\circ$ -2O unit cell, with O in the usual fcc hollow sites.<sup>33</sup> In this structure, each surface Rh atom has two oxygen neighbors, the same as for the O-stabilized Rh adatoms. The oxygen coverage in this oxygen adsorption structure ( $1.1 \times 10^{19}$  m<sup>-2</sup>) is higher than that in the RhO<sub>2</sub> monomer phases; nevertheless, the DOS of the RhO<sub>2</sub> monomer is clearly more oxide-like than metallic and even shows a dip where the fully developed bulk oxide has its band gap. The nonzero DOS at

the Fermi level is comparable to that of bulk RhO<sub>2</sub> (see SI) and has been also proposed for selected surface terminations of Rh<sub>2</sub>O<sub>3</sub>.<sup>34</sup> We may therefore name this structure a 0D oxide, in analogy to the 1D and 2D oxides already mentioned.

Further support for a difference of character between mere adsorption structures and the 0D oxide comes from an analysis of the charge transfer from a Rh atom to the neighboring oxygen atoms determined on the basis of a Bader analysis (Figure 4a). It is evident that even for the Rh<sub>2</sub>O<sub>3</sub> bulk oxide the effective charge transfer of 1.22 e is only a fraction of the amount attributed to the formal Rh<sup>3+</sup> charge state, which is a common effect for transition-metal oxides.<sup>32</sup> It is also clear that the charge of a Rh atom strongly depends on the number of oxygen neighbors, which is six in Rh<sub>2</sub>O<sub>3</sub>, two in the monomer and  $(\sqrt{3} \times \sqrt{3})$ -2O structures, and one in the  $p(2 \times 1)$  structure. Among the structures with two O neighbors, Rh in the 0D oxide is clearly more ionic than the simple adsorption structure, and also, the oxygen charges underline this trend, with a value closer to Rh<sub>2</sub>O<sub>3</sub> than to the simple  $(\sqrt{3} \times \sqrt{3})$ -2O adsorption structure.

Why is the formation of the 0D oxide on the Rh(113) surface favorable? It is well-known that metal atoms with lower coordination have higher reactivity; thus, oxygen is expected to bind more strongly to the Rh adatoms than to step atoms. In addition, favorable adsorption sites for the oxygen atoms in the 0D oxides help to compensate for the energy costs of having highly under-coordinated Rh adatoms at the surface (Figure 2). The upper O adatoms binding to each Rh adatom are in three-fold fcc sites, the most stable site on extended Rh(111) terraces.<sup>33</sup> Without any distortion of the Rh lattice, the lower O atoms would be in a four-fold hollow site with one Rh atom missing. Relaxation, that is, mainly a shift of the Rh adatom parallel to the step, also converts this site into a pseudo-three-fold site, similar to the distortion induced by O on Rh(100).<sup>35</sup> From the viewpoint of the Rh atoms, having two O adatoms at opposite sides is an especially favorable configuration ( $d_{z^2}$  bonding; cf. ref 36). Although the O atoms are not exactly at opposite sides for this structure, altogether, the stronger Rh–O bonding in the Rh adatom structure compared to a simple O overlayer compensates for the energy cost of breaking two Rh–Rh bonds required to create a single Rh adatom. The O–Rh–O angles are found to be 155, 152, and 144° for the mono-1, the mono-2, and the dim-6O, respectively. These values are significantly different from 180°, but the same is true for the 165° bond angle in bulk Rh<sub>2</sub>O<sub>3</sub>.

To our knowledge, the stabilization of single metal adatoms after oxygen exposure has not been reported in the literature so far. However, surface roughening driven by different adsorbates, such as upon CO exposure, has been observed on Pt(110)<sup>37</sup> as well as on vicinal surfaces,<sup>38</sup> including the formation of Pt adatoms. CO must be considered special, however, due to its very strong preference for low coordination of the metal atom to which it binds, culminating in the easy formation of highly volatile carbonyls of some transition metals, a property not shared by transition-metal oxides (with the exception of OsO<sub>4</sub>). Restructuring including adatom formation was also observed for surfaces of “softer” metals, such as Cu, exposed to organic molecules.<sup>39,40</sup> Obviously, the energy needed to restructure the surface of a more weakly bound metal is much lower than that for a refractory metal such as rhodium.

Although a few of the details of the mechanism of stabilizing the Rh adatoms seem to be rather specific for the current surface, much of the reasoning explaining the stability of the 0D oxide would apply to other transition-metal surfaces as well, for

example, bonding to opposite atoms via  $d_{z^2}$ -like orbitals or a preference for oxygen for fcc hollow sites. We thus consider it likely that stabilization of atoms with low coordination is not restricted to CO/Pt(110) and O/Rh(113), but we expect this to be a more general feature of open metal surfaces exposed to reactive gases. Finally, our study indicates that nanoparticles used in catalysis do not only change their shapes through interaction with a reactant gas,<sup>20</sup> but also the atomic arrangement on the nanofacets is strongly influenced by adsorption, accompanied by a change of bonding and electronic structure, already at surprisingly low gas pressures.

## ■ ASSOCIATED CONTENT

**§ Supporting Information.** Additional information and figures. This material is available free of charge via the Internet at <http://pubs.acs.org>.

## ■ AUTHOR INFORMATION

### Corresponding Author

\*E-mail: schmid@iap.tuwien.ac.at.

### Present Addresses

<sup>§</sup>Department of Physics, University of Central Florida, Orlando, Florida 32816, United States.

<sup>¶</sup>ESRF, 6, rue Jules Horowitz, F-38043 Grenoble Cedex, France.

## ■ ACKNOWLEDGMENT

This work was financially supported by the Swedish Research Council, the Crafoord Foundation, the Knut and Alice Wallenberg Foundation, the Anna and Edwin Berger Foundation, the Austrian Science Fund (FWF; projects S90 and F45), and the European Union under Contract No. NMP3-CT-2003-505670 (NANO2).

## ■ REFERENCES

- (1) Hendriksen, B L M; Frenken, J. W. M. CO Oxidation on Pt(110): Scanning Tunneling Microscopy Inside a High-Pressure Flow Reactor. *Phys. Rev. Lett.* **2002**, *89*, 046101.
- (2) Ackermann, M. D.; Pedersen, T. M.; Hendriksen, B. L. M.; Robach, O.; Bobaru, S. C.; Popa, I.; Quiros, C.; Kim, H.; Hammer, B.; Ferrer, S.; Frenken, J. W. M. Structure and Reactivity of Surface Oxides on Pt(110) during Catalytic CO Oxidation. *Phys. Rev. Lett.* **2005**, *95*, 255505.
- (3) Hendriksen, B L M; Bobaru, S C; Frenken, J W M. Oscillatory CO Oxidation on Pd(1 0 0) Studied with In-Situ Scanning Tunneling Microscopy. *Surf. Sci.* **2004**, *552*, 229–242.
- (4) van Rijn, R.; Balmes, O.; Felici, R.; Gustafson, J.; Wermeille, D.; Westerström, R.; Lundgren, E.; Frenken, J. W. M. Comment on CO Oxidation on Pt-Group Metals from Ultrahigh Vacuum to Near Atmospheric Pressures. 2. Palladium and Platinum. *J. Phys. Chem. C* **2010**, *114*, 6875–6876.
- (5) Gustafson, J.; Westerström, R.; Mikkelsen, A.; Torrelles, X.; Balmes, O.; Bovet, N.; Andersen, J. N.; Baddeley, C. J.; Lundgren, E. Sensitivity of Catalysis to Surface Structure: The Example of CO Oxidation on Rh under Realistic Conditions. *Phys. Rev. B* **2008**, *78*, 045423.
- (6) Gustafson, J.; Westerström, R.; Resta, A.; Mikkelsen, A.; Andersen, J. N.; Balmes, O.; Torrelles, X.; Schmid, M.; Varga, P.; Hammer, B.; Kresse, G.; Baddeley, C. J.; Lundgren, E. Structure and Catalytic Reactivity of Rh Oxides. *Catal. Today* **2009**, *145*, 227–235.
- (7) Gustafson, J.; Westerström, R.; Balmes, O.; Resta, A.; van Rijn, R.; Torrelles, X.; Herbschleb, C. T.; Frenken, J. W. M.; Lundgren, E. Catalytic Activity of the Rh Surface Oxide: CO Oxidation over Rh(111) under Realistic Conditions. *J. Phys. Chem. C* **2010**, *114*, 4580–4583.
- (8) Westerström, R.; Wang, J. G.; Ackermann, M. D.; Gustafson, J.; Resta, A.; Mikkelsen, A.; Andersen, J. N.; Lundgren, E.; Balmes, O.; Torrelles, X.; Frenken, J. W. M.; Hammer, B. Structure and Reactivity of a Model Catalyst Alloy under Realistic Conditions. *J. Phys.: Condens. Matter* **2008**, *20*, 184018.
- (9) Over, H.; Kim, Y. D.; Seitsonen, A. P.; Wendt, S.; Lundgren, E.; Schmid, M.; Varga, P.; Morgante, A.; Ertl, G. Atomic-Scale Structure and Catalytic Reactivity of the RuO<sub>2</sub>(110). *Surf. Sci.* **2000**, *287*, 1474–1476.
- (10) He, Y. B.; Knapp, M.; Lundgren, E.; Over, H. Ru(0001) Model Catalyst under Oxidizing and Reducing Reaction Conditions: In-Situ High-Pressure Surface X-ray Diffraction Study. *J. Phys. Chem. B* **2005**, *109*, 21825–21830.
- (11) Carlsson, P. A.; Zhdanov, V. P.; Skoglundh, M. Self-Sustained Kinetic Oscillations in CO Oxidation over Silica-Supported Pt. *Phys. Chem. Chem. Phys.* **2006**, *8*, 2703–2706.
- (12) Newton, M. A.; Dent, A. J.; Diaz-Moreno, S.; Fiddy, S. G.; Jyoti, B.; Evans, J. Rapid Monitoring of the Nature and Interconversion of Supported Catalyst Phases and of Their Influence upon Performance: CO Oxidation to CO<sub>2</sub> by  $\gamma$ -Al<sub>2</sub>O<sub>3</sub> Supported Rh Catalysts. *Chem.—Eur. J.* **2006**, *12*, 1975–1985.
- (13) Chen, M. S.; Cai, Y.; Yan, Z.; Gath, K. K.; Axnanda, S.; Goodman, D. W. Highly Active Surfaces for CO Oxidation on Rh, Pd, and Pt. *Surf. Sci.* **2007**, *601*, 5326–5331.
- (14) Zambelli, T.; Wintterlin, J.; Trost, J.; Ertl, G. Identification of the “Active Sites” of a Surface-Catalyzed Reaction. *Science* **1996**, *273*, 1688–1690.
- (15) Honkala, K.; Hellman, A.; Remediakis, I. N.; Logadottir, A.; Carlsson, A.; Dahl, S.; Christensen, C. H.; Nørskov, J. K. Science Ammonia Synthesis from First-Principles Calculations. *Science* **2005**, *307*, 555–558.
- (16) Gustafson, J.; Resta, A.; Mikkelsen, A.; Westerström, R.; Andersen, J. N.; Lundgren, E.; Weissenrieder, J.; Schmid, M.; Varga, P.; Kasper, N.; Torrelles, X.; Ferrer, S.; Mittendorfer, F.; Kresse, G. Oxygen-Induced Step Bunching and Faceting of Rh(553): Experiment and Ab Initio Calculations. *Phys. Rev. B* **2006**, *74*, 35401.
- (17) Westerström, R.; Gustafson, J.; Resta, A.; Mikkelsen, A.; Andersen, J. N.; Lundgren, E.; Seriani, N.; Mittendorfer, F.; Schmid, M.; Klikovits, J.; Varga, P.; Ackermann, M. D.; Frenken, J. W. M.; Kasper, N.; Stierle, A. Oxidation of Pd(553): From Ultrahigh Vacuum to Atmospheric Pressure. *Phys. Rev. B* **2007**, *76*, 155410.
- (18) Wang, J. G.; Li, W. X.; Borg, M.; Gustafson, J.; Mikkelsen, A.; Pedersen, T.; Lundgren, M.; Weissenrieder, E.; Klikovits, J.; Schmid, M.; Hammer, B.; Andersen, J. N. One-Dimensional PtO<sub>2</sub> at Pt Steps: Formation and Reaction with CO. *Phys. Rev. Lett.* **2005**, *95*, 256102.
- (19) Klikovits, J.; Schmid, M.; Merte, L.; Varga, P.; Westerström, R.; Resta, A.; Andersen, J.; Gustafson, J.; Mikkelsen, A.; Lundgren, E.; Mittendorfer, F.; Kresse, G. Step-Orientation-Dependent Oxidation: From 1D to 2D Oxides. *Phys. Rev. Lett.* **2008**, *101*, 266104.
- (20) Mittendorfer, F.; Seriani, N.; Dubay, O.; Kresse, G. Morphology of Mesoscopic Rh and Pd Nanoparticles under Oxidizing Conditions. *Phys. Rev. B* **2007**, *76*, 233413.
- (21) Klikovits, J.; Schmid, M.; Gustafson, J.; Mikkelsen, A.; Resta, A.; Lundgren, E.; Andersen, J. N.; Varga, P. Kinetics of the Reduction of the Rh(111) Surface Oxide: Linking Spectroscopy and Atomic-Scale Information. *J. Phys. Chem. B* **2006**, *110*, 9966–9975.
- (22) Gustafson, J.; Mikkelsen, A.; Borg, M.; Lundgren, E.; Köhler, L.; Kresse, G.; Schmid, M.; Varga, P.; Yuhara, J.; Torrelles, X.; Quirós, C.; Andersen, J. N. Self-Limited Growth of a Thin Oxide Layer on Rh(111). *Phys. Rev. Lett.* **2004**, *92*, 126102.
- (23) Gustafson, J.; Mikkelsen, A.; Borg, M.; Andersen, J. N.; Lundgren, E.; Klein, C.; Hofer, W.; Schmid, M.; Varga, P.; Köhler, L.; Kresse, G.; Kasper, N.; Stierle, A.; Dosch, H. Structure of a Thin Oxide Film on Rh(100). *Phys. Rev. B* **2005**, *71*, 115442.
- (24) Kresse, G.; Hafner, J. Ab Initio Molecular Dynamics for Liquid Metals. *Phys. Rev. B* **1993**, *47*, 558.
- (25) Kresse, G. Furthmüller Efficiency of Ab-Initio Total Energy Calculations for Metals and Semiconductors Using a Plane-Wave Basis Set. *J. Comput. Mater. Sci.* **1996**, *6*, 15–50.

- (26) Blöchl, P. E. Projector Augmented-Wave Method. *Phys. Rev. B* **1994**, *50*, 17953.
- (27) Kresse, G.; Joubert, D. From Ultrasoft Pseudopotentials to the Projector Augmented-Wave Method. *Phys. Rev. B* **1999**, *59*, 1758.
- (28) Perdew, J. P.; Chevary, J. A.; Vosko, S. H.; Jackson, K. A.; Pederson, M. R.; Singh, D. J.; Fiolhais, C. Atoms, Molecules, Solids, And Surfaces: Applications of the Generalized Gradient Approximation for Exchange and Correlation. *Phys. Rev. B* **1992**, *46*, 6671.
- (29) (a) Tang, W.; Sanville, E.; Henkelman, G. A Grid-Based Bader Analysis Algorithm without Lattice Bias. *J. Phys.: Condens. Matter* **2009**, *21*, 084204. (b) See also: <http://theory.cm.utexas.edu/bader/>.
- (30) Henkelman, G.; Arnaldsson, A.; Jonsson, H. A Fast and Robust Algorithm for Bader Decomposition of Charge Density. *Comput. Mater. Sci.* **2006**, *36*, 354–360.
- (31) Seriani, N.; Mittendorfer, F. Platinum-Group and Noble Metals Under Oxidizing Conditions. *J. Phys.: Condens. Matter* **2008**, *20*, 184023.
- (32) Raebiger, H.; Lany, S.; Zunger, A. Charge Self-Regulation upon Changing the Oxidation State of Transition Metals in Insulators. *Nature* **2008**, *453*, 763–766.
- (33) Köhler, L.; Kresse, G.; Schmid, M.; Lundgren, E.; Gustafson, J.; Mikkelsen, A.; Borg, M.; Yuhara, J.; Andersen, J. N.; Marsman, M.; Varga, P. High-Coverage Oxygen Structures on Rh(111): Adsorbate Repulsion and Site Preference Is Not Enough. *Phys. Rev. Lett.* **2004**, *93*, 266103.
- (34) Scherson, Y. D.; Aboud, S. J.; Wilcox, J.; Cantwell, B. J. Surface Structure and Reactivity of Rhodium Oxide. *J. Phys. Chem. C* **2011**, *115*, 11036–11044.
- (35) Baraldi, A.; Cerdá, J.; Martín-Gago, J. A.; Comelli, G.; Lizzit, S.; Paolucci, G.; Rosei, R. Oxygen Induced Reconstruction of the Rh(100) Surface: General Tendency Towards Threefold Oxygen Adsorption Site on Rh Surfaces. *Phys. Rev. Lett.* **1999**, *82*, 4874.
- (36) Lundgren, E.; Mikkelsen, A.; Andersen, J. N.; Kresse, G.; Schmid, M.; Varga, P. Surface Oxides on Close-Packed Surfaces of Late Transition Metals. *J. Phys.: Condens. Matter* **2006**, *18*, R481.
- (37) Thostrup, P.; Christoffersen, E.; Lorensen, H. T.; Jacobsen, K. W.; Besenbacher, F.; Nørskov, J. K. Adsorption-Induced Step Formation. *Phys. Rev. Lett.* **2001**, *87*, 126102.
- (38) Tao, F.; Dag, S.; Wang, L.-W.; Liu, Z.; Butcher, D. R.; Bluhm, H.; Salmeron, M.; Somorjai, G. A. Break-Up of Stepped Platinum Catalyst Surfaces by High CO Coverage. *Science* **2010**, *327*, 850–853.
- (39) Kreikemeyer Lorenzo, D.; Bradley, M. K.; Unterberger, W.; Duncan, D. A.; Lerotholi, T. J.; Robinson, J.; Woodruff, D. P. The Structure of Methoxy Species on Cu(110): A Combined Photoelectron Diffraction and Density Functional Theory Determination. *Surf. Sci.* **2011**, *605*, 193–205.
- (40) Rosei, F.; Schunack, M.; Jiang, P.; Gourdon, A.; Lægsgaard, E.; Stensgaard, I.; Joachim, C.; Besenbacher, F. Organic Molecules Acting as Templates on Metal Surfaces. *Science* **2002**, *296*, 328–331.